euronoise

Simulation of the oscillation dynamics and translational motion of ultrasound contrast agents

Alexander Teterev, Larisa Rudak and Natalia Misuchenko

Belarus State University, 4, Nezavisimosti Ave., 220030 Minsk, Belarus
teterev@bsu.by

A numerical model has been developed to simulate the oscillatory dynamics and the translational motion of both free and encapsulated bubbles in an ultrasound field. The model allows for the compressibility of the surrounding liquid and the bubble shell, which makes it possible to model the bubble dynamics at high acoustic pressures. Simulations can be carried out either by solving Rayleigh-Plesset-type equations, or in the hydrodynamic approximation taking into account the rheological properties of the liquid and the shell, or by a combined method. In the latter case, the gas pressure at the bubble surface, which is found from the gas-dynamic problem, is used as an input parameter for Rayleigh-Plesset-type equations at every time layer. The resulting radius of the bubble is then used as the boundary condition for the gas-dynamic equations. The model is a handy and flexible tool to investigate the effect of different factors on the oscillatory dynamics of the bubble, such as the thickness of the bubble shell, the rheological properties of the shell, and the translational displacement of the bubble. Using the developed model, the resonance frequency and translational displacement of contrast agents were numerically estimated.

1 Introduction

The wide application of ultrasound contrast agents in medicine [1] and progress of manufacturing techniques of new materials for encapsulating shells have given rise to intensive theoretical, numerical and experimental investigations in this field [2-3]. Of special interest are investigations on the effect of rheological behavior of shell materials on the radial dynamics of contrast agents in an ultrasound field. Depending on their material, encapsulating shells can exhibit the properties of a viscoelastic solid (KelvinVoigt solid), a viscoelastic fluid with stress relaxation (Maxwell fluid), as well as properties whose rheological law is still not understood. Buckling of lipid monolayer coatings is an example [4]. In [5], a model for large-amplitude oscillations of thin-shelled microbubbles has been developed. Theoretical analysis of small-amplitude oscillations of encapsulated bubbles with shell thickness exceeding 15 nm was carried out in [6]. The purpose of the present paper is to develop theoretical and numerical models that make it possible to examine different scenarios for the behavior of free and encapsulated bubbles in both small- and finite-amplitude ultrasound fields, taking adequate account of existent physical processes and to study the influence of rheological properties of a shell on the oscillatory dynamics and translation displacement of a ultrasound contrast agent.

2 Theoretical model

2.1 Model description

Depending on aims assigned, the proposed model allows one to carry out simulations in different ways. First, one can use one of systems of Rayleigh-Plesset-type equations built into the model. Second, one can make use of a combined method and simulate, for example, the gas flow within a free or contrast agent bubble using the gas-dynamic equations. In this case, the gas pressure at the bubble surface resulting from the gas-dynamic problem is an input parameter for Rayleigh-Plesset-type equations and the resulting radius and velocity of the surface of the bubble are then boundary conditions for the gas-dynamic equations. Finally, the third possibility is to model the gas dynamics inside the bubble, the dynamics of the shell if it is present, including a multilayer one, and the dynamics of the surrounding liquid using the hydrodynamic equations for a compressible medium and taking into account plasto-elastic, viscous, and even more complicated rheological properties of the encapsulating shell and the surrounding liquid. If a Rayleigh-Plesset-type equation is used, the gas motion is described by a polytropic equation, normally in the adiabatic approximation. The surrounding liquid is assumed to be compressible with a barotropic equation of state, such as the empiric Tait equation. It is also supposed that the surrounding liquid is at constant temperature and behaves as a Newtonian or a more complex fluid. The shell of the bubble is also at constant temperature, can be either compressible or incompressible, and its rheological behaviour can follow either a fluid or a solid. Mass transfer between the gas and the surrounding liquid (or the encapsulating layer) is assumed to be absent. Let us now consider the mathematical formulation of the problems, which is a set of ordinary differential equations and partial differential equations.

2.2 Rayleigh-Plesset-type model

In a free bubble case, the radial oscillation is calculated using Rayleigh-Plesset-type equations which are represented as a system of two ordinary differential equations of first order. The common form of the equations can written as

$$\dot{v} = F\left(R, v, X_n, Y_n, t\right), \quad v = \dot{R}, \tag{1}$$

where v is the radial velocity of the bubble surface, the over dot denotes the time derivative, R is the time-varying radius of the bubble, X_n is a set of parameters that describe the properties of the media such as viscosity, initial density, surface tension, sound speed, etc., Y_n is a set of parameters that describe the properties of the ultrasound field such as amplitude, frequency, etc., t is time.

As the main model of radial oscillation for contrast agents, which also takes into account translation, we use the model described in [7]. It can be represented as

$$\dot{v} = F\left(R, \delta R, v, v_x, D_i, \dot{D}_i, X_n, Y_n, x, t\right), \; v = \dot{R} \tag{2}$$

$$\dot{v}_x = F_x\left(R, \delta R, \dot{v}, v, X_n, Y_n, t\right), \quad v_x = \dot{x} \tag{3}$$

$$\dot{D}_i = F_i\left(D, R, \dot{v}, v, X_n\right), \tag{4}$$

where δR is the shell thickness, v_x is the translation velocity of the contrast agent, the function D_i is defined rheological behaviour of a medium, the subscript i = S for shell or L for surrounding liquid, x is the translation displacement of the contrast agent.

2.3 Hydrodynamic model

As the problem under consideration is one-dimensional, it is reasonable to solve it using the Lagrangian method. The continuity equation, written in Lagrangian mass coordinates, for the case of spherical symmetry, and with respect to density per unit spatial angle, takes the form [8]

$$\frac{\partial}{\partial t}\left(\frac{1}{\rho}\right)=\frac{\partial\left(ur^2\right)}{\partial m}, \tag{5}$$

where ρ and u are the density and the velocity of the gas, shell or surrounding liquid, respectively, and the relation between the Euler and the mass coordinates is given by $dm = \rho r^2 dr$. The equation of motion in the Lagrangian coordinates is written as

$$\frac{\partial u}{\partial t}=-r^2\frac{\partial p}{\partial m}+r^2\frac{\partial S_{rr}}{\partial m}+\frac{3S_{rr}}{r\rho}, \tag{6}$$

where p is the pressure, S_{rr} is the radial component of the stress deviator, $S_{rr} = 0$ for the gas. The energy equation in this case is given by

$$\frac{\partial}{\partial t}\left(\varepsilon+\frac{u^2}{2}\right)=-\frac{\partial}{\partial m}\left(r^2pu\right)+\frac{\partial}{\partial m}\left(r^2S_{rr}u\right), \tag{7}$$

where ε is the internal energy per unit mass.

2.4 State and rheology equations

To close the systems of Eq.(1), Eqs.(2)-(4), or Eqs.(5)-(7), state equations for the gas inside the bubble, the ambient liquid, and the bubble shell should be specified. Our model allows one to apply different variants of such equations. The gas motion can be described by the state equation of ideal gas, the Van der Waals equation, or a tabular equation of state. For the ambient liquid, the hydrodynamic equation of a compressible fluid can be used, as well as the empiric Tait equation of state or different tabular equations of state. Similar equations can also be used for the bubble shell. The choice of a specific set of state equations is determined by extreme values of gas-dynamic parameters that are achieved under conditions of interest.

To close the systems of Eqs.(2)-(4), or Eqs.(5)-(7), rheology equations for the surrounding liquid, and the bubble shell should be specified. For a viscoelastic plastic solid, S_{rr} and the viscous stress tensor q_{rr} are given by [9]

$$\frac{\partial S_{rr}}{\partial t}=-2\mu_i\left(\frac{\partial u}{\partial r}+\frac{1}{3\rho}\frac{\partial\rho}{\partial t}\right), \tag{8}$$

$$q_{rr}=2\eta_i\left(\frac{\partial u}{\partial r}+\frac{1}{3\rho}\frac{\partial\rho}{\partial t}\right), \tag{9}$$

where μ_i is the shear modulus and η_i is the shear viscosity for the liquid or the shell. If $|S_{rr}|\geq 2/3 Y_0$, than

$$S_{rr}=\frac{2}{3}Y_0\cdot sign\left(S_{rr}\right)+q_{rr}, \tag{10}$$

where Y_0 is the yield stress. For a viscoelastic fluid, S_{rr} is specified by the Oldroyd equation [10]

$$\lambda_{i1}\frac{\partial S_{rr}}{\partial t}+S_{rr}=2\eta_i\left(u_{rr}+\lambda_{i2}\frac{\partial u_{rr}}{\partial t}\right), \tag{11}$$

where $u_{rr} = \partial u/\partial r$ denotes the radial component of the rate-of-strain tensor, λ_{i1} is the relaxation time and λ_{i2} is the retardation time. For a viscoelastic fluid of the Maxwell model, S_{rr} is specified by

$$\lambda_{iM}\frac{\partial S_{rr}}{\partial t}+S_{rr}=2\eta_i u_{rr}, \tag{12}$$

where λ_{iM} is the relaxation time. For a viscoelastic solid, S_{rr} is specified by the Kelvin-Voigt equation

$$S_{rr}=2\mu_S\left(\varepsilon_{rr}+\lambda_{SV}u_{rr}\right), \tag{13}$$

where ε_{rr} is the radial component of the strain tensor, λ_{SV} is the retardation time for a shell.

3 Numerical model

3.1 Solving the systems of ODE

To solve systems of Eq.(1) or Eqs.(2)-(4), our model uses different calculation methods. For example, when these systems are solved in combination with the gas-dynamic equations, the Euler methods can be applied as a consequence of small time step used by the gas-dynamic equations. For more complicated cases, the Runge-Kutta-Gill method with accumulating error checking and automatic time step selection can be applied [11]. At mean accuracy of solution, the best result is reached using the Runge-Kutta method based on Dormand's and Prince's formulas with automatic step length control [12]. The set of methods used for solving ODE can be widened, which allows one to control the accuracy of solutions and the validity of results obtained.

3.2 Solving the systems of hydrodynamic equations

The hydrodynamic equations for the gas inside the bubble, as well as for the bubble shell and the ambient liquid, are solved by the completely conservative method described in [13]. The calculation of the stress tensor deviators describing the rheological behaviour of the shell and the ambient liquid is carried out using the technique proposed in [9]. As the solved system of equations is implicit, the solution was found by means of iterations, the termination criterion being the convergence condition of total energy for all points of the area under consideration.

3.3 Capabilities of the model and its notification

To establish the correspondence between a result and a scenario that was used to obtain that result, the following notation of the model scenarios is introduced: $MN_I^T(A)$. The first letter is always M, which denotes "Model". N can be 0, 1, or 2. 0 means that the result was obtained using a model based on a Rayleigh-Plesset-type equation. 1 denotes that the combined method was used, where the gas flow inside the bubble is calculated by the gas-dynamic model and the radius of the bubble is calculated by a Rayleigh-Plesset-type equation. Finally, 2 designates that all results

were obtained by the hydrodynamic simulation. The subscript I can be B, S, or M. B denotes that the dynamics of a free bubble is considered, S indicates an encapsulated bubble, and M denotes that the bubble shell is multilayer. If the superscript T is present, that means that the calculation was made taking into account translation. The model author's name or its abbreviation can be given in the parentheses. Thus, $M1_S$(D) denotes that the results were obtained for an encapsulated bubble taking into account the gasdynamic flow inside a bubble, and the radial oscillation was calculated by the Doinikov model [7].

4 Numerical simulations

4.1 Resonance frequencies

An example of the calculation of translational displacement of a contrast agent bubble for different driving frequencies is given in Fig.1. The translational displacement is shown as a function of resting bubble radius for five frequencies. The simulation was carried out using the model $M0_S^T$(D). The shell thickness is assumed to be constant and equal to 2 nm, the shell density is 1100 kg/m^3, the pulse duration is 20 cycles, and the frequencies are 1.5, 2, 2.5, 3, and 4 MHz. The ambient liquid is water at the atmospheric pressure. The acoustic pressure amplitude is 200 kPa. The viscosity of water η_L is 0.001 Pa·s, the shell viscosity η_S is 1.0 Pa·s, and the shell relaxation time λ_{S1} is $1.25\cdot10^{-8}$·s. In addition, marks on each curve show points that correspond to resonance radii calculated by two different methods for each frequency. Triangles show resonance radii that are calculated on the basis of the resonance frequency of a free bubble. Circles represent resonance bubble radii that are determined from oscillation power plots. The algorithm of this approach was proposed in [7]. For a specified driving frequency, the equilibrium bubble radius is determined at which the oscillation power function

$$W(f,R_0)=1/T\int_0^T\left(R(t)/R_0-1\right)^2 dt \qquad (14)$$

where T is the duration of the imposed acoustic pulse, reaches a maximum.

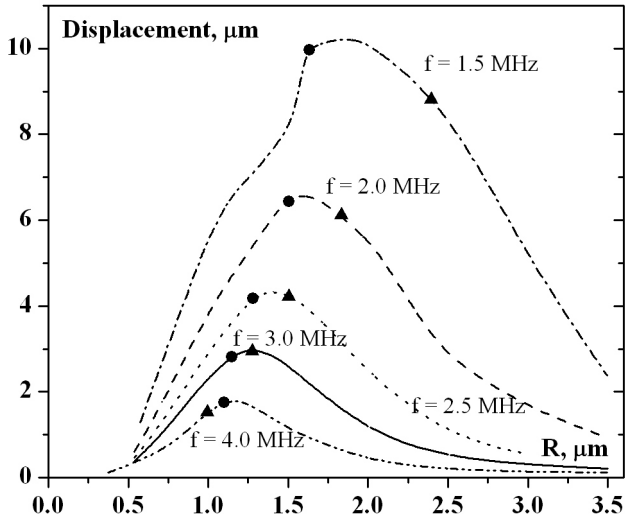

.Fig.1 Translation displacement as a function of resting bubble radius.

Comparison between the radii of contrast agents for which the maximal displacement occurs at a given frequency, and the resonance radii marked on the curves shows that the translational displacement can also be a measure that determines the resonance frequency of a contrast agent.

4.2 Thick shells

In order to study the effect of rheological properties of a shell on the oscillatory dynamics and translational displacement of a contrast agent, calculations were made for various rheological models. The simulation was carried out using the model $M2_S^T$. The Maxwell fluid model, Eq.(12), the 3-constant Oldroyd model, Eq.(11), and the elasto-plastic model, Eqs.(8)-(10), were used. As a contrast agent, an air bubble with radius R_0 = 1 μm and a shell of thickness δR_0 = 0.1 μm, density ρ_{0S} = 1100 kg/m^3 and shell viscosity η_S = 0.01 Pa·s was taken. The parameters of the surrounding liquid were the same as in the preceding tasks. The oscillation dynamics of the contrast agent is shown in Fig.2 for three cycles of an ultrasound signal with a frequency of 2 MHz. In the Maxwell model, shown by the solid line, the relaxation time λ_{SM} is 10^{-9}s. The relaxation times for the Oldroyd model were set to be equal to λ_{S1} = 10^{-8}s and λ_{S2} = 10^{-11}s. In Fig.2, this model is shown by the dotted line. Finally, the dashed line represents the elasto-plastic model with the shear modulus G = 10^8Pa and the yield stress Y_0 = 0.7 MPa.

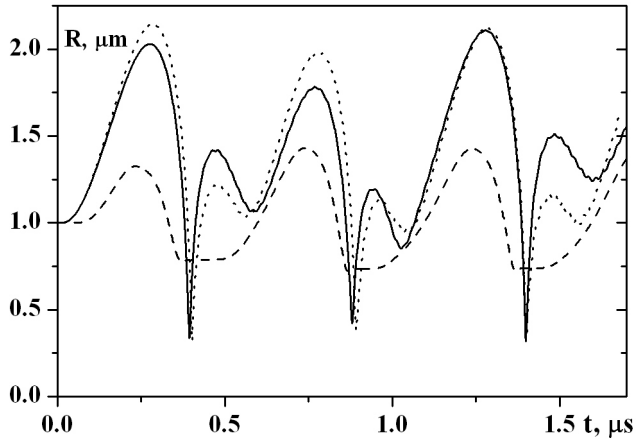

.Fig.2 The time-dependent radius of a contrast agent for three variants of rheological laws.

The behavior of the contrast agent with the shell described by the Maxwell and Oldroyd models is virtually identical. However, the translational displacement shown in Fig.3 exhibits a difference in their dynamics. The elasto-plastic shell leads to smooth small-amplitude oscillations of the contrast agent (see Fig.2) and as a consequence to the smallest translational displacement among all the tested variants (see Fig.3).

Calculation was also performed for a shell described by the Voigt solid model. However, on the scale shown in Fig.2, oscillations in this case are unnoticeable, and the time dependence of the radius is just a straight line. A similar result is also obtained for the elasto-plastic shell if the ultimate strength of the shell material exceeds 1 MPa.

Figure 3 displays the dynamics of translational displacement of contrast agents for the same variants of

computation. It is seen that the observed difference in the oscillatory dynamics due to different rheological properties of the shells results in a considerable difference in displacement.

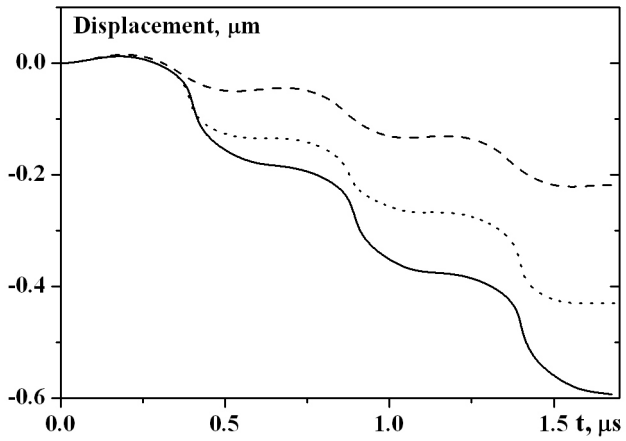

.Fig.3 Simulated translational displacement as a function of time for three cycles of an ultrasound signal.

For the model parameters which were used in the calculations, the largest displacement is reached for the Maxwell fluid shell (solid line). Whereas the smallest displacement is observed for the elasto-plastic shell (dashed line). However, by varying the model parameters, one can obtain other ratios between translational displacements. This fact suggests that one can formally select such parameter values that any model can be fitted to experiment. Therefore, to get plausible results, it is important to estimate the model parameters from experimental data.

4.3 Thin shells

Of special interest are currently contrast agents with ultrathin monolayer lipid shells. Description of the properties of such shells is complicated as the shells may exhibit different aggregative states at the water-air interface. Indeed, at strong rarefaction, they behave as a perfect two-dimensional gas which at compression demonstrates the properties of a stretched liquid film. Even stronger compression leads to a condensed liquid film and finally results in a virtually incompressible solid condensed state [14]. Further compression leads to shell buckling. To describe such a shell, it is natural to assume that its behavior is smoothly changing from a gas state to a liquid and then solid state. During this process the surface tension and the shell viscosity will undergo corresponding changes.

To investigate the suitability of different rheological models to a lipid shell, three variants of calculation were carried out. In the first variant, the Maxwell fluid model was used, in the second, the Voigt solid model, and the third variant was a combination of these two models and was based on the above described mechanism of transformation of lipid monolayers. Let us assume that the rearrangement of a monomolecular lipid layer is realized by a smooth transition from a solid condensed state to a liquid film and then backwards. As in the case of spherical symmetry the rarefaction occurs at the expansion of a contrast agent, the shell being getting thinner, while the compression occurs when the bubble radius is decreasing, the shell being getting thicker, the conditions of rarefaction and compression can be related directly to the shell thickness. This approach can be described by the following equation for the rate of the stress deviator in the terms of respective quantities for the Maxwell and Voigt models:

$$\dot{S} = \alpha \dot{S}_V + (1-\alpha)\dot{S}_M \quad 0 \le \alpha \le 1 \qquad (15)$$

where S_V is the stress deviator of the Voigt model and S_M is the stress deviator of the Maxwell model. The parameter α can be related to the shell thickness as follows. Let us divide the entire range of the shell thickness into 5 regions. In the first region, at $0 < h < h_1$, the shell behaves as a perfect gas, while at $h_1 < h < h_2$, it behaves as a Maxwell fluid. If the shell thickness lies in the range $h_2 < h < h_3$, then a smooth transition from the calculation by the Maxwell fluid model, Eq.(12), to that by the Voigt solid model, Eq.(13), is performed, and then backwards using Eq.(15) with α given by

$$\alpha = (h-h_2)/(h_3-h_2), \quad h_2 \le h \le h_3 \qquad (16)$$

In the range $h_3 < h < h_4$, the shell behaves as a Voigt solid, while at $h \ge h_4$, the shell breaks down with nulling of the stresses which existed before.

Shell thicknesses obtained in the course of the simulation of the oscillation dynamics and the translational motion of the contrast agent are depicted in Fig.4. The simulation was carried out by the model $M2_S^T$. The initial shell thickness is equal to 2 nm, the shell density is 1100 kg/m^3, the pulse duration is 2 cycles, and the frequency is 4 MHz, the acoustic pressure amplitude is 200 kPa. The shell relaxation time λ_{S1} is 10^{-8}·s for Eq.(12) and the shell retardation time λ_{SV} is 10^{-11}·s for Eq.(13), the shell viscosity η_S is 1.0 Pa·s. The ranges boundaries of shell thickness for Eq.(16) are equal 0.2, 1.4, 1.8, 3 nm. Note that in the calculation made by our model (solid line), the change in the shell thickness for the time period considered is minimal and virtually coincides with the change in the shell thickness obtained by the Voigt model (dashed line). At the same time, the difference between the maximum and minimum radii of the contrast agent for our model is maximal. This occurs because the main contribution to this difference comes from the maximum attainable size of the contrast agent. While this contribution to the change of the shell thickness, as compared to the other models, is not so great.

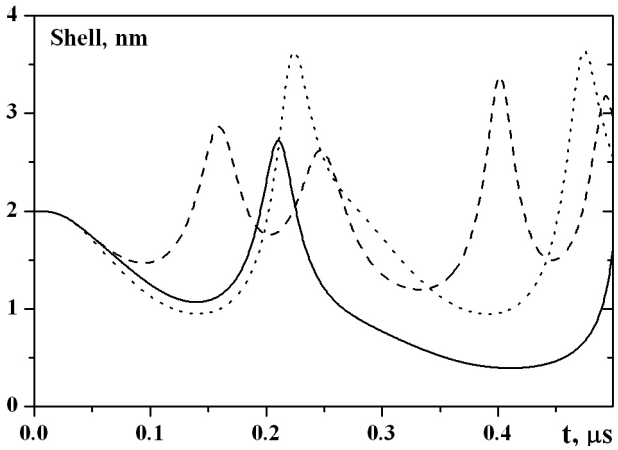

.Fig.4 Simulated shell thickness as a function of time.

Figure 5 shows translational displacement of contrast agents as a function of time for different shell models. As is

the case with thick shells, the largest displacement is reached for the Maxwell fluid model (dotted line), while the smallest one is observed for the Voigt model (dashed line). Our model proposed here has an intermediate value in this case.

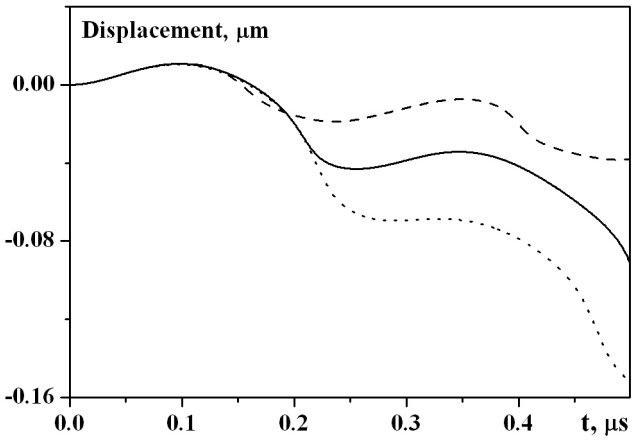

.Fig.5 Simulated translational displacement as a function of time for two cycles of an ultrasound signal.

5 Conclusion

The developed model is a logical extension and improvement of the model proposed in [15]. The present model makes it possible to consider a wide circle of problems on the dynamics of free and contrast agent bubbles in both weak and strong ultrasound fields. It involves the calculation of translational displacement of contrast agents and the determination of their resonance frequencies. It makes possible both widening the circle of numerical simulations on oscillations of free gas bubbles in liquids in response to an imposed strong ultrasound field and solving similar problems for encapsulated bubbles with different rheological models for the encapsulating shell.
The model also allows one to apply different rheological laws to the surrounding liquid, which makes possible the simulation of more complicated media than Newtonian fluids, such as blood. In the hydrodynamic approximation, a bubble with a multilayer coating can be investigated. The implementation of the described model is a handy and flexible tool for simulating various aspects of the oscillatory dynamics of free and contrast agent bubbles.

Acknowledgments

This work was supported by the US member of the International Science and Technology Center (ISTC) under Contract B-1213.

References

[1] S. L. Mulvagh, A.N. DeMario, S.B. Feinstein et al., “Contrast echocardiography: current and future applications”, *J. Am. Soc. Echocardiography*, 13(4), 331-342 (2000)

[2] A. A. Doinikov, (ed). Bubble and Particle Dynamics in Acoustic Fields: Modern Trends and Applications, Research Signpost: Kerala, India (2005)

[3] J. Chomas, P. Dayton, D. May, K. Ferrara, “Nondestractive subharmonic imaging”, *IEEE Trans. Ultrason, Ferroelect., Freg. Contr.*, 49(7), 883-891 (2002)

[4] M. Borden, G. Pu, G. Runner, M. Longo, “Surface phase behavior and microstructure of lipid/PEG-emulsifier monolayer-coated microbubbles”, *Colloids and Surfaces B*, 35, 209–223 (2004)

[5] P. Marmottant, S. van der Meer, M. Emmer, M. Versluis, N. de Jong, S. Hilgenfeldt, D. Lohse, “A model for large amplitude oscillations of coated bubbles accounting for buckling and rupture”, *J. Acous. Soc. Am.*, 118(6), 3499–3505 (2005)

[6] D. B. Khismatullin, A. Nadim, “Radial oscillations of encapsulated microbubbles in viscoelastic liquids. Physics of Fluids”, 14(10), 3534–3557 (2002)

[7] A .A. Doinikov, P. A. Dayton, “Nonlinear dynamics of lipid-shelled ultrasound microbubble contrast agents”, Computational methods in multiphase flow IV, WIT Press Southampton, Boston, 261-270 (2007)

[8] Y. B. Zeldovitch, Yu. Raiser, Physics of Shock Waves and High-Temperature Hydrodynamic Phenomena, Academic: New York (1967)

[9] C. L. Mader, Appendix A and B, Numerical modeling of detonations, University of California Press (1985)

[10] R. B. Bird, R. C.Armstrong, O. Hassager, Dynamics of polymeric liquids, Wiley: New York (1987)

[11] E. S. Oran, J. P. Boris, Numerical simulation of reactive flow, ELSEVIER, New York – Amsterdam – London (1987)

[12] E. Hairer, S. P. Norsett, G. Wanner, Solving ordinary differential equations nonstiff problems, Springer-Verlag: Berlin and New York (1987)

[13] A. A. Samarsky, J .P. Popov, Difference methods for solving gas dynamic equations, Nauka: Moscow (1980)

[14] A. B. Rubin, Biophysics, book 2, Biophysics of cell processes, Moscow (1987)

[15] A. V. Teterev, N. I. Misychenko, L. V.Rudak, A. A. Doinikov, “Simulation of radial oscillations of a free and a contrast agent bubble in an ultrasound field,” Computational methods in multiphase flow IV, WIT Press Southampton, Boston, 239-248 (2007)